PHYSICAL REVIEW B **81**, 081202(R) (2010)

Unraveling effects of disorder on the electronic structure of SiO_2 from first principles

Layla Martin-Samos, Giovanni Bussi, Alice Ruini, and Elisa Molinari
National Center on nanoStructures and bioSystems at Surfaces, INFM-CNR-S3, I-41100 Modena, Italy
and Dipartimento di Fisica, Università di Modena e Reggio Emilia, I-41100 Modena, Italy

Marília J. Caldas
Instituto de Física, Universidade de São Paulo, 05508-900 São Paulo, SP, Brazil

(Received 15 October 2009; revised manuscript received 1 December 2009; published 2 February 2010)

We present a first-principles systematic study of the electronic structure of SiO_2 including the crystalline polymorphs α quartz and β cristobalite, and different types of disorder leading to the amorphous phase. We start from calculations within density functional theory and proceed to more sophisticated quasiparticle calculations according to the *GW* scheme. Our results show that different origins of disorder have also different impact on atomic and electronic-density fluctuations, which affect the electronic structure and, in particular, the size of the mobility gap in each case.

DOI: 10.1103/PhysRevB.81.081202 PACS number(s): 72.20.Ee, 71.10.−w, 71.23.−k

In amorphous semiconductors and insulators the free-carrier transport is directly related to the so-called mobility gap, defined as the energy difference between mobility edges separating localized states tails from extended band states.[1] The mobility edges are thus the relevant energies for the real values of band offsets at interfaces, and the mobility gap plays for the amorphous material the same role as the electrical energy gap in crystalline systems. From the experimental side, the values reported for the measured mobility gap of amorphous silica (a-SiO_2) exhibit a broad dispersion. However, experimental studies agree in that they do not show marked differences between a-SiO_2 and α quartz,[2,3] the most common SiO_2 crystalline polymorph. This experimental evidence is however counterintuitive in that the density of a-SiO_2 is smaller than that of quartz, and we should thus expect a closure of the gap as for other tetrahedral compounds. On the other hand, besides the technological interest, amorphous forms of silicon dioxide appear as natural prototypes for network-forming disordered materials. The theoretical interpretation of transport and optical properties of amorphous semiconductors or insulators in terms of mobility edges[1] and localized (Urbach) tails derives from the pioneering ideas of Anderson, Mott and Cohen,[4–7] and we could suppose that the opening of the gap of a-SiO_2 is totally coming from extreme localization of band-edge states, i.e., formation of Urbach tails. Most theoretical results so far that lead to such interpretations addressed model systems through simplified Hamiltonians containing parametrized terms to account for the disorder contribution; calculations on model structures obtained through tight-binding mean-field treatments[8,9] or *ab initio* density functional theory (DFT) methods[10] and applied to the study of the electronic structure of amorphous silica are also usually compared to crystalline α quartz, and suggest a smaller mobility gap. First-principles beyond-mean-field methods, based on many-body perturbation theory (MBPT), have been applied more recently to the study of optical properties separately for the crystalline systems quartz[11] and cristobalite.[12,13]

In the present work, we go beyond the previous studies by investigating through the same methodology different crystalline polymorphs, α quartz and β-cristobalite (Fd-3m), and several amorphous models of SiO_2 having different kinds and degrees of disorder. We start from the generation of reasonably large silica models and heated crystal structures through classical simulations[14] of quench from the melt, proceed through full first-principles electronic structure calculations within *ab initio* DFT formalism, and reach the calculation of the quasiparticle electronic structures within MBPT by means of the *GW* approach.[15]

We distinguish[16] thermal disorder, where the connectivity of the crystalline-phase network is preserved, and just bond lengths and angles are affected, from topological disorder where also the number of atoms in a connectivity ring is affected. We find that at the fundamental gap edges the two kinds of disorder mainly touch the upmost valence band, and lead to different effects. Still at the mean-field level, we see a slight gap closing in the thermal, and a strong gap opening in the topological disorder case. For the more realistic well-quenched samples, we find just a small spreading of Urbach tails at the valence-band edge: the effect on the size of the gap is mostly brought about by band flattening and narrowing due to orbital localization. This orbital localization leads also to different many-body corrections on the level energies, which are larger for the disordered systems than for the coherent crystalline phases, and contribute to the final almost coincidence of the mobility gap value for a-SiO_2 and α quartz.

We use a 108 atom supercell for crystalline α quartz, and the 24 atom primitive cell for β cristobalite. To distinguish between topological and thermal-like disorder, we also investigate the heating of the cristobalite crystal up to 300 K, which provides a test case where only short-range disorder associated to small fluctuations plays a role, and in this case we adopt a 192 atom supercell. The amorphous systems are investigated through four a-SiO_2 models, that are all made of connected SiO_4 tetrahedra: at the short-range scale, differences between the two crystalline and the amorphous systems come from bond-angle and bond-length fluctuations, while the medium-range structure is governed by the connectivity of the SiO_4 network itself.[17] We performed molecular-dynamics (MD) simulations of quenching from a melt using a semiempirical ionic potential[18,19] in order to generate four

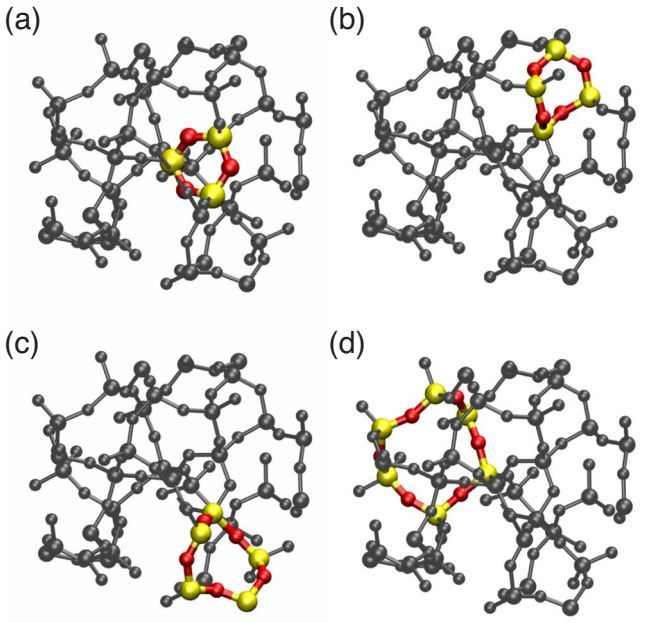

FIG. 1. (Color online) Topological structure of the WQ1 silica model: the ring-size distribution is made evident by recognizing the presence of 3- to 6-membered rings, respectively, in panels (a)–(d).

108 atom glasslike configurations for silica with different degrees of disorder. Two of them are "well-quenched" (labeled WQ1 and WQ2), since they have been prepared following the procedure described in Ref. 14 with an effective quench rate of 2.6×10^{13} K/s: they are well connected in the sense of Zachariasen;[17] the other two ("fast-quenched," labeled FQ1 and FQ2) have been prepared just by standard procedure with an effective quench rate of 1.1×10^{15} K/s. These latter two models show different network characteristics: the first (FQ1) matches the well-connected network definition, while the other has a defective network with an edge-sharing tetrahedra (FQ2). As shown in Fig. 1, the medium-range structure pertaining to the amorphous silica models generated by our MD simulations presents a variety of small-ring connections, including 3- and 4-membered rings, which is also consistent[20] with the interpretation of Raman experiments. All structures have been fully relaxed, through first-principles DFT calculations in the local density approximation (LDA). Our calculations were performed[21] using norm-conserving pseudopotentials and plane-wave expansions up to 70 Ry. The many-body electronic structure for each model was then obtained by performing nonself-consistent *GW* calculations.[22–25]

One of the key concepts for understanding the role of disorder in amorphous semiconductors and insulators is the distinction between localized and extended electronic states, which is still under debate.[26] We here quantitatively describe localization by means of a new tool, i.e., a normalized self-interaction ($|\mathrm{SI}|$). The self-interaction is the Coulomb interaction between an electronic state and itself $(=\frac{1}{V}\int\int \frac{\phi_s^*(r)\phi_s(r)\phi_s^*(r')\phi_s(r')}{\|r-r'\|}d^3rd^3r')$, and we further extend this concept to systems modeled through periodic boundary conditions by dividing the usual SI by the SI of a plane wave normalized in the corresponding cell. This normalized SI

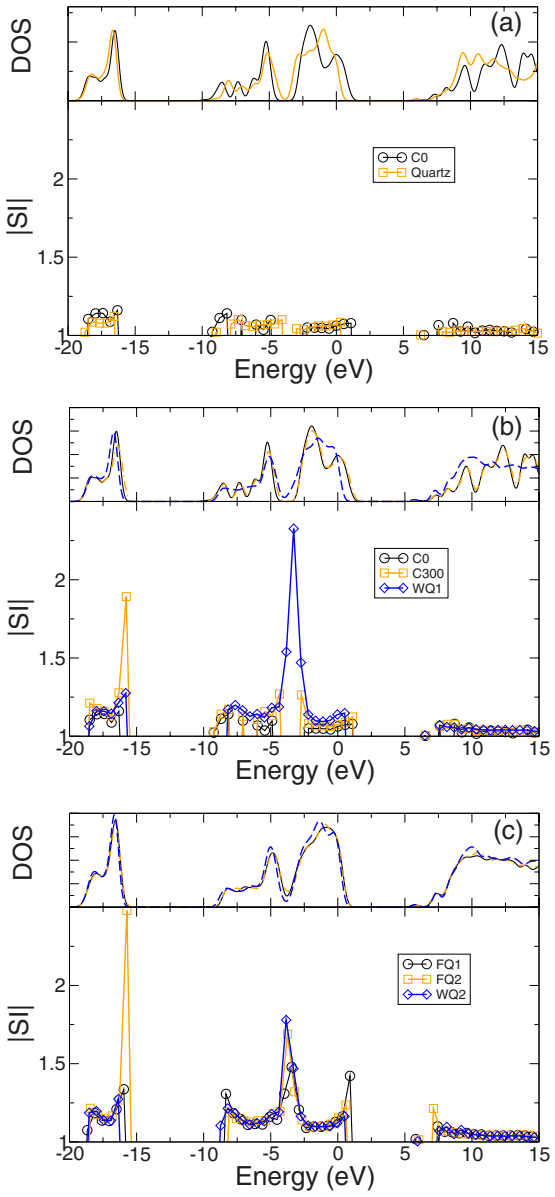

FIG. 2. (Color online) DOS and normalized self-interaction for the DFT-LDA states of (a) cristobalite C_0 and quartz at 0 K, (b) cristobalite at 0 K, at 300 K C_{300} and the WQ1 silica model, and (c) silica models FQ1, FQ2, and WQ2. The DOS are plotted with a Gaussian broadening of 0.27 eV, and have been aligned by the bottom of the valence band. The reported $|\mathrm{SI}|$ is averaged over energy intervals of 0.09 eV.

provides us with an absolute quantification of localization, which is independent of the energy, and can be used to compare the localization in systems with different unit-cell volumes [a fully delocalized state will always exhibit a $|\mathrm{SI}|$ value of one, while a completely localized state, a Dirac's delta, will have a divergent $|\mathrm{SI}|$ (Ref. 27)].

We examine first in detail the DFT-LDA results. We show in Fig. 2 the density of states (DOS) and corresponding $|\mathrm{SI}|$ for (a) the two crystals at 0 K; (b) for the systems with the same density, i.e., cristobalite at 0 and 300 K, and the WQ1 system; and (c) for the WQ2, FQ1 and FQ2 systems. The density of all the investigated systems is reported in the first

TABLE I. Density, HOMO-LUMO gap (E_{HL}), and mobility gap (E_μ) of crystalline and glass models within the DFT-LDA and *GW* approaches: α quartz (Q) and β cristobalite at 0 and 300 K (C_0 and C_{300}); well-quenched (WQ), and fast-quenched (FQ) amorphous models, see text. Densities are given in g/cm^3, energies in eV.

	Q	C_0	C_{300}	WQ1	WQ2	FQ1	FQ2
Density	2.65	2.20	2.20	2.18	2.27	2.44	2.40
E_{HL} (DFT)	5.9	5.4	5.3	5.6	5.6	5.3	5.2
E_μ (DFT)	5.9	5.4	5.3	5.7	5.7	5.6	5.5
E_μ (*GW*)	9.4	8.9		9.6	9.4	9.2	9.1
Δ_{xc}	3.5	3.5		3.9	3.7	3.6	3.6

row of Table I. Figure 2 shows that all the DOS exhibit a roughly similar shape, with not enough information on the amorphous or crystalline character of the system except for the dip in the DOS between bonding and nonbonding states (at about −5.0 eV) that is less pronounced in the amorphous case; this is also observed experimentally[28] according to the degree of frozen-in disorder. The behavior of the |SI| coupled to the DOS is however very elucidative. Indeed, our |SI| results for the amorphous models show that the states energetically located at the dip (related according to Ref. 28 to the local fluctuations in the short-range order, such as bond-angle distortions and bond dimerization) have a strongly localized character. Coming to the top of the valence band, the analysis of |SI| reveals that the fast-quenched models clearly exhibit highly localized tails, with a concentration of the order of 10^3-10^4 ppm.[29] Moreover, a careful inspection of |SI| data reveals that the physics at the band edge is rather complex and system dependent, which precludes a widespread definition of mobility edges to be applied to any disordered sample. For example, for silica our results show that disorder does not produce any localized state in the lower conduction bands, while strongly influencing the valence bands: the 2*p* oxygen states are significantly perturbed by disorder, differently from those silicon-related states involved in generating lower conduction states. The absence of localization for unoccupied states was already suggested in Ref. 20, and we remark that our |SI| results allow to recognize that the LUMO states for these systems are completely delocalized: their very nature is unaffected by any kind of disorder.

Focusing at the upper valence band, we see that overall the value of |SI| for the amorphous samples is higher than for the crystalline phases, including the thermally disordered cristobalite.[30] We calculate the mobility gap as the energy difference between conduction and valence mobility edges, defined as the first state having a |SI| value larger than 1.12, i.e., the largest |SI| value found at the same band for cristobalite, the crystalline reference of a-SiO_2 with the same density. The DFT and *GW* results for the mobility gap for all systems are summarized in Table I, where the corresponding density and highest occupied molecular orbital lowest unoccupied molecular orbital (HOMO-LUMO) gap within DFT are also reported (for a crystalline system at 0K the DFT mobility and HOMO-LUMO gaps coincide). In the case of ordered systems, both the DFT and the *GW* calculations indicate the closure of the direct gap for lower-density systems, i.e., cristobalite wrt quartz. This result is in agreement with the well-known interplay between gap and density in crystalline semiconductors and insulators, and it also corresponds to the trend extracted from experiments addressing the optical gap of tetrahedral systems.[31] The comparison between C_0 and C_{300} shows that thermal disorder induces a slight narrowing of the gap, without any particularly strong localization of the band-edge states. Passing now to the effect of topological disorder, Table I indicates that the mobility gap of well-quenched amorphous systems, calculated through DFT or *GW*, is always larger than the corresponding-density crystal gap. A similar behavior has been observed in Ref. 9 opposing the effect of weak and strong disorder for model tetrahedral systems. The case of fast-quenched samples is more complex, since the value of the density by itself is not enough to describe the morphology effect; the systems we analyze here are highly inhomogeneous, and lower-density phases coexist with higher-density defect regions. However, the DFT mobility gap is again larger than that of cristobalite, and we find a wider energy interval of localized tails compared to the well-quenched samples.

The inclusion of many-body corrections produces the expected opening of the gap. The self-energy correction turns out to be exactly the same for the two crystalline systems (3.5 eV). A rationale for this behavior can be provided by analysis of the structural features of the two structures: according to the network characterization of King,[32] cristobalite is composed by 6-membered SiO_4 rings, while quartz displays 6- and 8-membered rings. Therefore, the insensitivity of the *GW* correction with respect to the cases of quartz and cristobalite suggests that the spatial range of the dominant nonlocal interactions controlling the gap is of the order of the 6-membered ring radius. Coming now to the amorphous phases, Table I shows that they all experience a larger correction, of up to 3.9 eV, owing to the sensitivity of the *GW* self-energy to the nonlocal-density fluctuations related to their topological disorder; as shown in Fig. 1, the silica models generated by our MD simulations present a variety of ring connections, including 3- and 4-membered rings, and the presence of small-numbered rings induces an enhancement of the local atomic density in the medium-range scale, which differentiate a-SiO_2 from the crystalline phases. The experimentally observed identity of the electronic properties of quartz and a-SiO_2 is not really captured by the DFT calculations, however the different corrections affecting crystalline and amorphous phases allow us to recover the agreement with the experiments indicating that a-SiO_2 and quartz

phases are indistinguishable in spectroscopic experiments. Their mobility gap is around 9.4–9.6 eV,[33] within the reported experimental range (8.8–11.5 eV[2,34]) and in very good agreement with, for instance, photoconductivity measurements 9.3 eV.[35] We also remark that the difference between *GW* corrections for crystalline and amorphous systems precludes an *a priori* use of crystalline shifts (within scissor shift approximations) for describing many-body contributions in disordered systems.

In summary, we succeeded in defining a consistent criterium to define the mobility gap of amorphous silica, based on the concept of normalized self-interaction, and in calculating it from first principles: our result is in very good agreement with matching experiments, and this is only possible through the explicit inclusion of many-body effects in the description of the electronic properties of crystalline and amorphous systems. The systematic character of our study allows us to follow the effects of atomic- and electronic-density fluctuations on the electronic structure, in particular the size of the mobility gap, and to discriminate the specific contribution of the different kinds of disorder: in the short-range scale, thermal fluctuations affecting bond distances and angles induce a gap narrowing, while the stronger, topological disorder tends to widen it. As expected on the basis of the Anderson model, we find that any kind of disorder may induce electron localization at band tails, with a localization that growth exponentially within the tails: however, these localized states hardly influence the mobility gap for realistic systems.

We are grateful to Carlo Cavazzoni, Andrea Ferretti, Guido Roma, and Yves Limoge for fruitful discussion. Computer time was mainly provided by CINECA through CNR-INFM Parallel Computing Projects. The support by RTN EU Contract "EXCITING" No. HPRN-CT-2002-00317 and by FIRB-MIUR Italy-Canada Grant No. RBIN06JB4C is acknowledged. M.J.C. acknowledges support from FAPESP and CNPq.

[1] E. N. Economou and M. H. Cohen, Phys. Rev. B **5**, 2931 (1972).
[2] P. Van den Keybus and W. Grevendonk, Phys. Rev. B **33**, 8540 (1986).
[3] K. Saito and A. J. Ikushima, Phys. Rev. B **62**, 8584 (2000).
[4] P. W. Anderson, Phys. Rev. **109**, 1492 (1958).
[5] M. H. Cohen, H. Fritzsche, and S. R. Ovshinsky, Phys. Rev. Lett. **22**, 1065 (1969).
[6] P. Anderson, Phys. Rev. Lett. **34**, 953 (1975).
[7] N. F. Mott, Rev. Mod. Phys. **50**, 203 (1978).
[8] J. Sarnthein, A. Pasquarello, and R. Car, Phys. Rev. Lett. **74**, 4682 (1995).
[9] F. Fazileh, X. Chen, R. J. Gooding, and K. Tabunshchyk, Phys. Rev. B **73**, 035124 (2006).
[10] T. Koslowski, W. Kob, and K. Vollmayr, Phys. Rev. B **56**, 9469 (1997).
[11] E. K. Chang, M. Rohlfing, and S. G. Louie, Phys. Rev. Lett. **85**, 2613 (2000).
[12] L. E. Ramos, J. Furthmuller, and F. Bechstedt, Phys. Rev. B **69**, 085102 (2004).
[13] R. Shaltaf, G.-M. Rignanese, X. Gonze, F. Giustino, and A. Pasquarello, Phys. Rev. Lett. **100**, 186401 (2008).
[14] L. Martin-Samos, Y. Limoge, J.-P. Crocombette, G. Roma, N. Richard, E. Anglada, and E. Artacho, Phys. Rev. B **71**, 014116 (2005).
[15] L. Hedin and S. Lundqvist, Solid State Phys. **23**, 1 (1969).
[16] D. Weaire and M. F. Thorpe, Phys. Rev. B **4**, 2508 (1971).
[17] W. H. Zachariasen, J. Am. Chem. Soc. **54**, 3841 (1932).
[18] B. W. H. van Beest, G. J. Kramer, and R. A. van Santen, Phys. Rev. Lett. **64**, 1955 (1990).
[19] We used Ewald sums for the bare Coulomb potential and a cutoff of 5.5 Å for the short-range part of BKS potential as explained in Ref. 36.
[20] A. Pasquarello and R. Car, Phys. Rev. Lett. **80**, 5145 (1998).
[21] P. Giannozzi *et al.*, J. Phys.: Condens. Matter **21**, 395502 (2009).
[22] L. Martin-Samos and G. Bussi, Comput. Phys. Commun. **180**, 1416 (2009).
[23] R. W. Godby and R. J. Needs, Phys. Rev. Lett. **62**, 1169 (1989).
[24] R. Del Sole, L. Reining, and R. W. Godby, Phys. Rev. B **49**, 8024 (1994).
[25] Within a convergence of 0.1 eV for general energy differences, while the fundamental energy-gap value is converged within 0.02 eV.
[26] Y. Song, W. A. Atkinson, and R. Wortis, Phys. Rev. B **76**, 045105 (2007).
[27] To avoid Coulomb divergence, we employ the reciprocal space correction introduced in Ref. 37 as discussed in Ref. 22.
[28] A. Di Pomponio, A. Continenza, L. Lozzi, M. Passacantando, S. Santucci, and P. Picozzi, Solid State Commun. **95**, 313 (1995).
[29] Concentration calculated as the number of localized states divided by the total number of occupied states.
[30] We use temperature as an artificial way to introduce a small stochastic perturbation to bond lentgh and bond angles.
[31] A. R. Goni, K. Syassen, and M. Cardona, Phys. Rev. B **39**, 12921 (1989).
[32] S. V. King, Nature (London) **47**, 3053 (1967).
[33] The experimental quenching rates are usually much smaller than $\simeq 10^{13}$ K/s; therefore, WQ1 and WQ2 are more meaningfully compared to experiments than FQ1 and FQ2.
[34] R. Evrard and A. N. Trukhin, Phys. Rev. B **25**, 4102 (1982).
[35] Z. A. Weinberg, G. W. Rubloff, and E. Bassous, Phys. Rev. B **19**, 3107 (1979).
[36] K. Vollmayr, W. Kob, and K. Binder, Phys. Rev. B **54**, 15808 (1996).
[37] F. Gygi and A. Baldereschi, Phys. Rev. B **34**, 4405 (1986).